THE JOURNAL OF BIOLOGICAL CHEMISTRY
Vol. 271, No. 7, Issue of February 16, pp. 3627–3632, 1996

*Printed in U.S.A.*

# Cooperative Oxygen Binding to *Scapharca inaequivalvis* Hemoglobin in the Crystal*

(Received for publication, June 20, 1995, and in revised form, October 2, 1995)

**Andrea Mozzarelli, Stefano Bettati, Claudio Rivetti, and Gian Luigi Rossi**

*From the Istituto di Scienze Biochimiche, Università di Parma, 43100 Parma, Italy*

**Gianni Colotti and Emilia Chiancone**

*From the Centro Studio sulla Biologia Molecolare, Dipartimento di Scienze Biochimiche A. Rossi Fanelli, Università di Roma La Sapienza, Piazzale Aldo Moro 5, 00185 Roma, Italy*

**Oxygen binding to homodimeric *Scapharca inaequivalvis* hemoglobin (HbI) crystals has been investigated by single-crystal polarized absorption microspectrophotometry. The saturation curve, characterized by a Hill coefficient $n_H$ = 1.45 and an oxygen pressure at half saturation $p_{50}$ = 4.8 torr, at 15 °C, shows that HbI in the crystalline state retains positive cooperativity in ligand binding. This finding will permit the correlation of the oxygen-linked conformational changes in the crystal with the expression of cooperativity.**

**Polarized absorption spectra of deoxy-HbI, oxy-HbI, and oxidized HbI crystals indicate that oxygenation does not induce heme reorientation, whereas oxidation does. Lattice interactions prevent the dissociation of oxidized dimers that occurs in solution and stabilize an equilibrium distribution of pentacoordinate and hexacoordinate high spin species.**

The study of the homodimeric, cooperative hemoglobin from the clam *Scapharca inaequivalvis*, HbI,[1] has suggested a mechanism of cooperativity in oxygen binding that is radically different from that operative in HbA. The mechanism is based on the comparison of the deoxy- and liganded HbI crystal structures, determined in orthorhombic and monoclinic crystals, respectively, and entails prominent tertiary changes in the heme environment but only subtle quaternary changes (1–4). Communication between the heme groups via localized structural changes is made possible by the unusual assembly of the globin chains. In HbI, the heme-carrying E and F helices form the dimer interface (5) rather than being exposed to solvent as in HbA. Thereby, the heme groups are brought into nearly direct contact through a network of hydrogen bonds, which is modified upon oxygenation (2–5).

In order to establish whether the crystal structures of HbI fully correlate with function in solution, we asked the question whether cooperative oxygen binding is retained by the protein in the crystalline state. In fact, it cannot be excluded, *a priori*, that crystallization conditions favor a protein conformation different from that prevailing in solution and that lattice interactions restrict its activity-related movements. The functional behavior has been commonly used as a stringent criterion to compare structural properties of proteins in solution and in the crystalline state (6–9).

The response of crystals of human hemoglobin A (HbA) to oxygenation exemplifies the delicate interplay between intramolecular rearrangements associated with ligand binding and intermolecular interactions stabilizing the crystal. Deoxy-HbA crystals, grown from high salt solutions, shatter in the presence of oxygen (10, 11), as lattice interactions neither prevent nor accommodate the T → R quaternary transition (12, 13). In contrast, deoxy-HbA crystals, grown from polyethylene glycol solutions, are stable when exposed to oxygen because the protein remains in the T quaternary state with intact salt bridges (14–16). A single crystal polarized absorption microspectrophotometric study has shown that oxygen binds noncooperatively to these crystals, saturating both $\alpha$ and $\beta$ hemes (17, 18). Similar studies have been carried out on stable crystals of Hb Rothschild (19) and des-Arg HbA (20).

Single-crystal polarized absorption microspectrophotometry is here exploited to determine oxygen binding curves to HbI crystals grown in the deoxy state. To obtain a precise estimate of the fractional saturation of reduced hemes, it is critical to evaluate exactly the amount of HbI molecules present in the oxidized form. The spectrum of soluble HbI in the oxidized state is pH-dependent and reflects an equilibrium distribution between two high spin dimeric components and a low spin monomeric hemichrome (21). Therefore, this equilibrium has been characterized in the crystalline state.

## MATERIALS AND METHODS

*Isolation, Purification, and Crystallization of HbI*—*Scapharca inaequivalvis* HbI was isolated and purified as described previously (22). Crystals of deoxy HbI were grown at room temperature by mixing deoxygenated 5 mM phosphate buffer, pH 8.0, containing 22 mg/ml HbI, and deoxygenated 3.5 M phosphate buffer, pH 8.5, as measured after calibration of the electrode with the standards 48 mM phosphate buffer, pH 7, and 50 mM carbonate buffer, pH 10. The final solution contained 30 mM sodium dithionite. Crystallization vials were deoxygenated and stored anaerobically. Crystals of size suitable for microspectrophotometric measurements (10–30 $\mu$m thick) grew in 1.8–2.0 M phosphate buffer as rhombic plates, belonging to the orthorhombic space group $C222_1$,[2] like the larger deoxy-HbI crystals grown for x-ray studies (2, 3).

*Oxygen Binding by HbI Crystals*—Individual crystals of deoxy HbI were withdrawn from a crystallization vial and were washed at least 6 times in 3.5 M phosphate buffer, pH 8.5, containing 1 mM EDTA and 0.35 mg/ml (20 units/$\mu$g) catalase (Sigma, bovine liver), in air. No crystal damage was observed during this procedure. Crystals were placed in a Dvorak-Stotler flow cell (23) and covered with an optically isotropic, gas permeable, silicon-copolymer membrane, MEM213

* This work was supported by funds from the Italian Ministry of Universities and Research in Science and Technology and from the Italian National Research Council Target Project on Biotechnology and Bioinstrumentation. The costs of publication of this article were defrayed in part by the payment of page charges. This article must therefore be hereby marked "*advertisement*" in accordance with 18 U.S.C. Section 1734 solely to indicate this fact.

[1] The abbreviations used are: HbI, dimeric *S. inaequivalvis* hemoglobin; HbA, human hemoglobin A; PR, polarization ratio.

[2] W. E. Royer, Jr., personal communication.

(General Electric). Helium-oxygen humidified gas mixtures were prepared with a computerized gas standard generator (Environics, series 200) and flown into the cell using 316 stainless steel tubing. Oxygen pressure at the outlet of the cell was determined by an oxygen meter equipped with a Clark electrode. The flow cell was mounted on the thermostatted stage of a Zeiss MPM03 microspectrophotometer.

Single crystal polarized absorption spectra were recorded between 450 and 700 nm. The electric vector of the incident polarized light was parallel either to the *a* or to the *b* crystal axis. These axes coincide with the diagonals of the plate and are principal optical directions of the crystal. Polarized light absorption along these directions obeys the Beer-Lambert law. The optical theory for myoglobin and hemoglobin crystals has been previously reported (18, 24, 25).

Oxygen binding curves were determined by recording polarized absorption spectra of HbI crystals equilibrated with either progressively increasing or progressively decreasing oxygen pressures, at 15 °C, as described previously (17, 18). The time required to obtain a stable spectrum of oxygenated HbI crystals depends on crystal thickness and oxygen pressure. For oxygen pressures below 2 torr, equilibration times for HbI crystals suitable for microspectrophotometric studies are of the order of days, and oxygen electrode drift precludes measurements. Long equilibration times also cause the unavoidable formation of oxidized HbI. For these reasons, even at higher oxygen pressures, each crystal was used for no more than three measurements.

*pH-dependent Spectral Changes of Oxidized HbI Crystals*—Oxidation of HbI crystals was achieved by suspending them in a solution containing 3.5 M potassium phosphate and 2 mM potassium ferricyanide for about 30 min. Polarized absorption spectra of oxidized HbI crystals were recorded after suspending the same crystal in 3.5 M potassium phosphate at different pH values.

*Solution Spectra of Oxidized HbI at High Salt Concentration*—Concentrated oxy-HbI in a solution containing 10 mM phosphate buffer, pH 7.0, was oxidized with potassium ferricyanide dissolved in the same buffer. The oxidized protein was subsequently concentrated to $4 \times 10^{-3}$ M (heme) with an Amicon Centricon 10 apparatus, thus eliminating the excess ferricyanide and the ferrocyanide formed during the redox reaction. The concentrated HbI solution was mixed in different ratios with 4 M potassium phosphate buffer, at pH values between 6.3 and 8.5, to yield a final phosphate concentration of 1–3 M. Absorption spectra were recorded between 450 and 700 nm by using a Varian Cary 3 spectrophotometer, at 15 °C. The pH of each solution was measured after spectral recording. It was not possible to determine spectra in the presence of phosphate concentrations higher than 3 M and of protein concentrations higher than $1 \times 10^{-3}$ M, nor to oxidize concentrated HbI in a high ionic strength buffer, due to protein precipitation.

*Data Analysis*—Fractions of deoxygenated, oxygenated, and oxidized hemes in HbI crystals were determined by a least squares fitting of the polarized spectra recorded in the presence of various oxygen pressures to a linear combination of deoxy-, oxy-, and oxidized HbI polarized spectra (reference spectra) (17, 18). Spectra of crystals containing oxidized HbI in proportions higher than 20% were not used for oxygen affinity determinations.

The pH-dependent absorption spectra of oxidized HbI in solution were analyzed with a singular value decomposition algorithm (Matlab, The Math Works Inc., Natick, MA) and fitted according to the equilibrium scheme given by Spagnuolo *et al.* (21), which describes the pH-dependent interconversion of three components, a dimeric hexacoordinate, a dimeric pentacoordinate, and a monomeric hemichrome.

The pH-dependent polarized absorption spectra of oxidized HbI in the crystal were fitted to a linear combination of the basis spectra of the three oxidized species in solution. The contributions of the different components to the observed polarized spectra $A_{obs}$ were calculated by the following expression:

$$A_{obs} = c_{Dh} \times A_{Dh} + c_{Dp} \times A_{Dp} + c_M \times A_M + c_{off} \times A_{off} \qquad \text{(Eq. 1)}$$

where $A_{Dh}$, $A_{Dp}$, and $A_M$ are the basis spectra in solution of the dimeric hexacoordinate, dimeric pentacoordinate, and monomeric hemichrome, respectively, and $c_{Dh}$, $c_{Dp}$, and $c_M$ are coefficients proportional to both the fractional concentration of the various species and their extinction coefficients along each crystal axis. $c_{off} \times A_{off}$ represents a horizontal offset. The use of the above expression is justified by the observation that the ratio of absorbances at each wavelength in the two perpendicular directions of polarization is almost constant, *i.e.* the electronic transitions are almost perfectly *x, y* polarized (18, 24, 25).

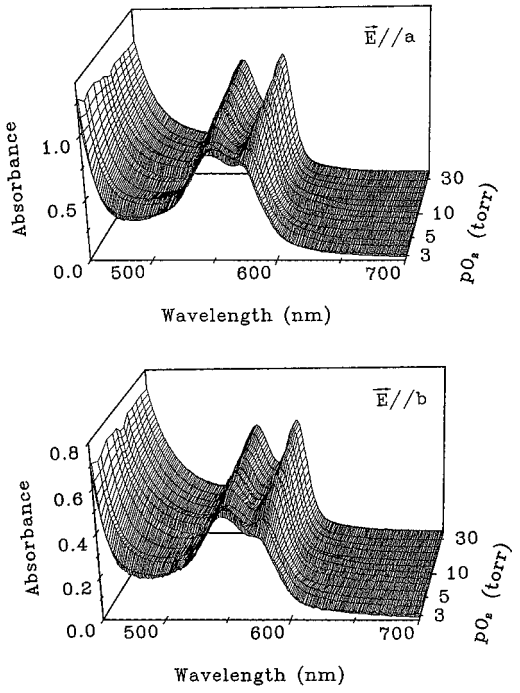


FIG. 1. **Single crystal polarized absorption spectra of HbI at different oxygen pressures.** Crystals of HbI, suspended in a solution containing 3.5 M potassium phosphate, 1 mM EDTA, 0.35 mg/ml catalase, pH 8.5, at 15 °C, were equilibrated with humidified oxygen mixtures between 2 and 37 torr. Polarized absorption spectra were recorded with the electric vector parallel either to the *a* or to the *b* crystallographic axis. Due to the long time required to equilibrate a crystal at low oxygen pressures, one crystal was used for no more than three measurements. Spectra of different crystals were normalized to the reference crystal spectra (see Fig. 2). Oxygen pressure is plotted on a log scale such that distances are proportional to chemical potentials.

## RESULTS

*Oxygen Binding by Crystals of HbI*—Single crystal polarized absorption spectra of HbI, recorded along the *a* and the *b* crystallographic axes, at oxygen pressures between 2 and 37 torr, at 15 °C (Fig. 1), indicate that HbI crystals bind oxygen reversibly and that oxygenation does not lead to crystal damage. In order to determine the fraction of oxygenated, deoxygenated, and oxidized hemes at different oxygen pressures, polarized absorption spectra of pure deoxy-, oxy-, and oxidized HbI (reference spectra) were obtained using the same crystal. First, a ferrous HbI crystal was fully oxidized by suspending it in a solution containing 2 mM potassium ferricyanide. Upon oxidation, fine crystal cracks transiently appear on the crystal surface. Thereafter, excess reagent was removed, and polarized spectra were recorded (Fig. 2*a*). The oxidized HbI crystal was then reduced by resuspending it in a solution containing 30 mM sodium dithionite, and spectra were recorded (Fig. 2*b*). Finally, the crystal was washed with a dithionite-free solution equilibrated with oxygen at a pressure of 760 torr. Polarized spectra were recorded and corrected for the presence of small amounts of oxidized protein (Fig. 2*c*). Since no appreciable spectral differences were observed by comparing spectra recorded at 160 and 760 torr, these spectra represent the absorption of fully oxygenated HbI crystals. An example of the least-squares fitting of the observed spectra in the presence of 5.5 torr of oxygen to a linear combination of the reference spectra and an offset is shown in Fig. 2*d*.

Hill plots of the data are shown in Fig. 3. The oxygen pressure required for half-saturation ($p_{50}$) is 4.9 ± 1.0 and 4.8 ± 0.8 torr, as determined from spectra recorded along the *a* and the *b* crystal axes, respectively. The Hill coefficient ($n_H$) deter-

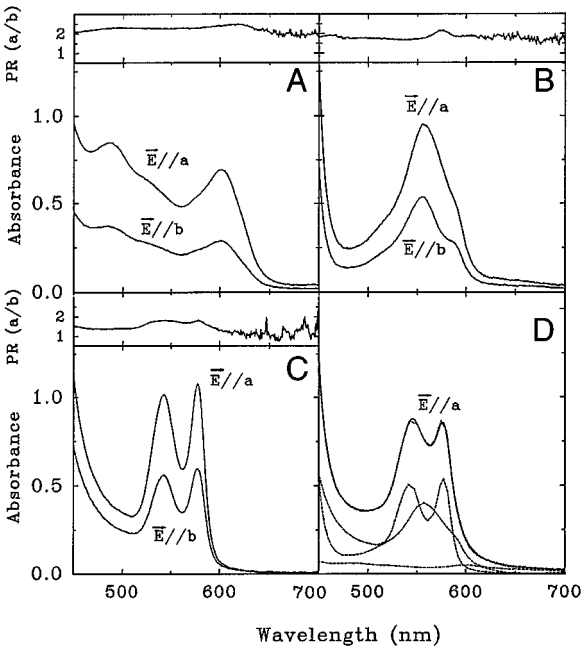


FIG. 2. **Single crystal polarized absorption spectra and polarization ratios of deoxy-HbI, oxy-HbI and oxidized HbI (reference spectra).** The spectra of oxidized HbI were recorded on a crystal, oxidized with 2 mM ferricyanide and then washed with 3.5 M potassium phosphate, pH 8.5 (*panel a*); the spectra of deoxy-HbI were obtained by suspending the same crystal in 30 mM dithionite (*panel b*); the spectra of oxy-HbI were obtained by resuspending the crystal, after removal of dithionite, in a solution equilibrated at 760 torr of oxygen (*panel c*). The contribution of a small fraction of oxidized HbI to the oxy-HbI spectra, as evidenced by a shoulder at 602 nm, was subtracted, and the spectra were properly normalized as described previously (18). For each set of spectra, the polarization ratio is plotted on the top portion of each panel. In *panel d*, the observed polarized spectrum, recorded with the electric vector parallel to the *a* crystal axis, at an oxygen pressure of 5.5 torr (——), is compared with that calculated from the fitting to a linear combination of the reference spectra (– – –), the fractional contribution of the spectra of deoxyHbI, oxyHbI, and oxidized HbI being 42.5, 50.1, and 7.4%, respectively. The fractional saturation with oxygen, defined as the ratio of oxygenated hemes over reduced plus oxygenated hemes, is 54.5%.

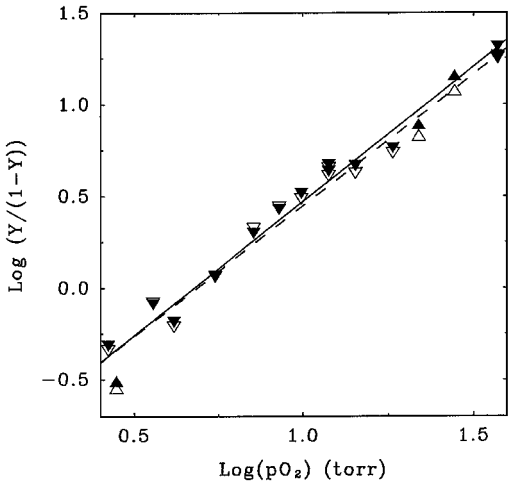


FIG. 3. **Hill plots of oxygen binding data for HbI crystals.** Crystals of HbI were suspended in 3.5 M potassium phosphate, 1 mM EDTA, pH 8.5, at 15 °C. The Hill coefficient $n_H$ and the $p_{50}$ are 1.43 ± 0.07 and 4.9 ± 1.0 torr, respectively, from data recorded along the *a* axis (*open symbols, dashed line*), and 1.46 ± 0.06 and 4.8 ± 0.8 torr from data recorded along the *b* axis (*closed symbols, solid line*), either by increasing (△, ▲) or decreasing (▽, ▼) the oxygen pressure.

TABLE I
*Projection of heme planes and polarization ratios in crystals of HbI*

| | $\sin^2 z_i a^a$ | $\sin^2 z_i b^a$ | $\sin^2 z_i c^a$ | $PR(A_{\|a}/A_{\|b})_{calc}{}^b$ | $PR(A_{\|a}/A_{\|b})_{obs}{}^c$ |
|---|---|---|---|---|---|
| deoxy-HbI | | | | | |
| heme 1 | 0.940 | 0.193 | 0.867 | | |
| heme 2 | 0.529 | 0.540 | 0.930 | | |
| $\Sigma_i \sin^2 z_i \mu$ | 1.469 | 0.733 | 1.797 | 2.0 | 1.79 |
| oxy-HbI | | | | | 1.81 |
| oxidized HbI (pH 8.5) | | | | | 2.40 |

[a] $z_i a$, $z_i b$, $z_i c$ are the angles between the normal to the plane of the *i* heme chromophore (taken as the *z* molecular axis) and the $\mu$ crystal axes *a*, *b*, and *c*. The plane of the heme was determined as the least squares best plane through the 24 porphyrin skeletal atoms, using the x-ray coordinates of HbI (2SDH.pdb from Brookhaven Data Bank).

[b] Calculated as $\Sigma_i \sin^2 z_i a / \Sigma_i \sin^2 z_i b$.

[c] Calculated as the ratio of absorbances at 556 nm for deoxy-HbI, 542 nm for oxy-HbI, and 602 nm for oxidized HbI.

mined from the two sets of data is 1.43 ± 0.07 and 1.46 ± 0.06, respectively. In solution, at 15.1 °C, in 0.1 M phosphate buffer, pH 7.8, the $p_{50}$ for HbI is 5.7 torr and the Hill coefficient is 1.44 (26).

Polarized absorption spectra of hemoglobin crystals provide information on the heme orientation in different ligation states (24, 25). The pertinent parameter is the polarization ratio (PR), *i.e.* the ratio of the absorbances in two perpendicular directions at wavelengths where the electronic transitions are almost perfectly *x*, *y* polarized. A good estimate of PR can be obtained by calculating the ratio of absorbances at 556 nm for deoxy-HbI and at 542 nm for oxy-HbI. The PR values ($A\|_a/A\|_b$) are 1.79 and 1.81 for deoxy- and oxy-HbI, respectively (Table I), indicating that oxygen binding is not accompanied by a heme tilt. This result is in agreement with the crystallographic finding that hemes have the same orientation in deoxy-HbI (2) as in CO-HbI (1, 3) and oxy-HbI crystals (4).

*pH Dependence of the Equilibrium Distribution of Oxidized Species in HbI Crystals*—Polarized absorption spectra of oxidized HbI crystals (Fig. 4*a*) and spectra of oxidized soluble HbI in 1–3 M phosphate buffer at millimolar protein concentrations (Fig. 4*b*) were recorded as a function of pH. For both sets of data, the pH-dependent spectral changes were analyzed in terms of three components, the hexacoordinate aquomet, the pentacoordinate species, and the hemichrome. Representative examples are given in Fig. 4, *c* and *d*. The most striking differences concern the monomeric hemichrome, which is practically absent in the crystalline state over the entire pH range examined (Fig. 5*a*). Thus, in the crystal, the spectra are a combination of the spectra of the pentacoordinate and the hexacoordinate dimeric species, with the latter component varying between 70 and 35% at pH values between 6.3 and 8.5. The contribution of the aquomet hexacoordinate species to absorption is consistently higher in the spectra recorded with light polarized along the *b* crystal axis, a result suggesting that in the two oxidized species, the hemes are differently oriented with respect to the crystal axes.

The calculated $pK_a$ for the transition between the two dimeric species is 7.07 ± 0.13 and 7.02 ± 0.11, as determined by polarized absorption spectra along the *a* and the *b* crystal axes, respectively (Fig. 4*a*, *inset*).

In solution, the hemichrome and the high spin hexacoordinate component are the predominant species under all the conditions investigated (Fig. 4*d* and Fig. 5, *b* and *c*). The amount of hemichrome decreases in the alkaline range with a concomitant increase of the pentacoordinate heme, whereas the

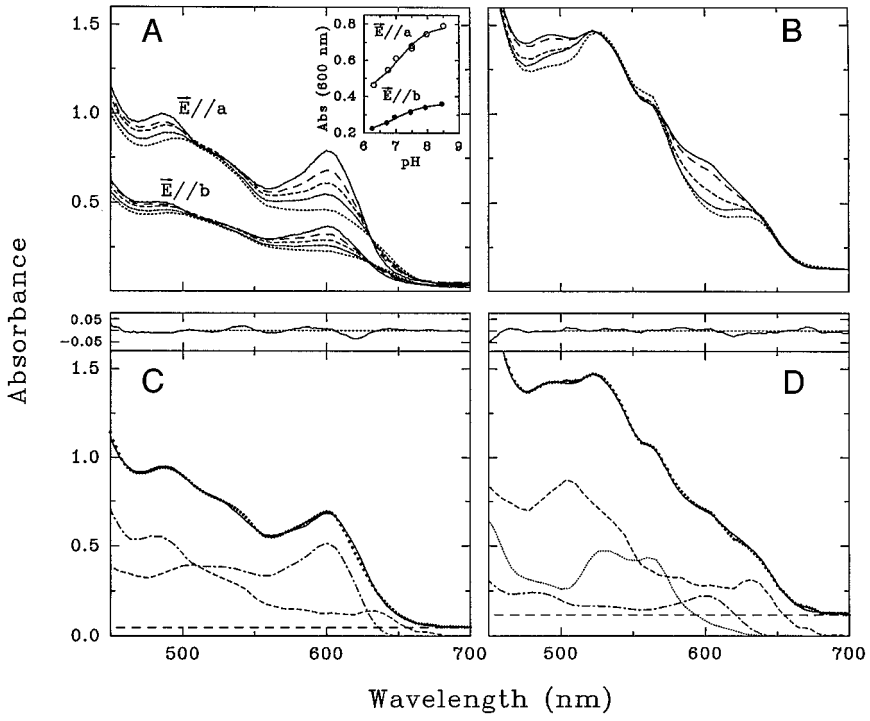


FIG. 4. **Dependence on pH of the spectra of oxidized HbI in the crystal and in solution.** *a*, a single crystal of oxidized HbI was suspended in a solution containing 3.5 M potassium phosphate at pH 6.3 (····), 6.8 (- - - -), 7.0 (– – –), 7.5 (— — —) and 8.5 (——). Polarized absorption spectra were recorded along the *a* and the *b* crystal axes. *Inset*, the absorbance change at 600 nm along the *a* (○) and the *b* axis (●) was fitted to the equation for the ionization of a group with p$K_a$ = 7.07 ± 0.13 and 7.02 ± 0.11, respectively. *b*, absorption spectra of 1 mM oxidized HbI in a solution containing 1 M potassium phosphate at pH 6.0 (····), 6.5 (- - - -), 7.0 (– – –), 7.5 (— — —), and 8.0 (——), at 15 °C. Spectra were normalized by subtraction of a horizontal offset (see *panel d*). The optical path was 1 mm. *c*, fitting of the oxidized HbI spectrum in the crystal at pH 7.5, recorded along the *a* axis (···), to a linear combination (——) of the spectra of high spin hexacoordinate (– – –), high spin pentacoordinate (–·–·–), low spin hemichrome species (not detectable), and an offset (— — —). The basis spectra are taken from Spagnuolo *et al.* (21). The residuals between observed and calculated spectra are reported in the top part of the panel. *d*, fitting of the spectrum of oxidized HbI in a solution containing 1 M potassium phosphate, pH 7.5 (···), to a linear combination (——) of the spectra of high spin hexacoordinate (– – –), high spin pentacoordinate (–·–·–), low spin hemichrome species (···) and an offset (— — —) (21). The residuals between observed and calculated spectra are reported in the top part of the panel.

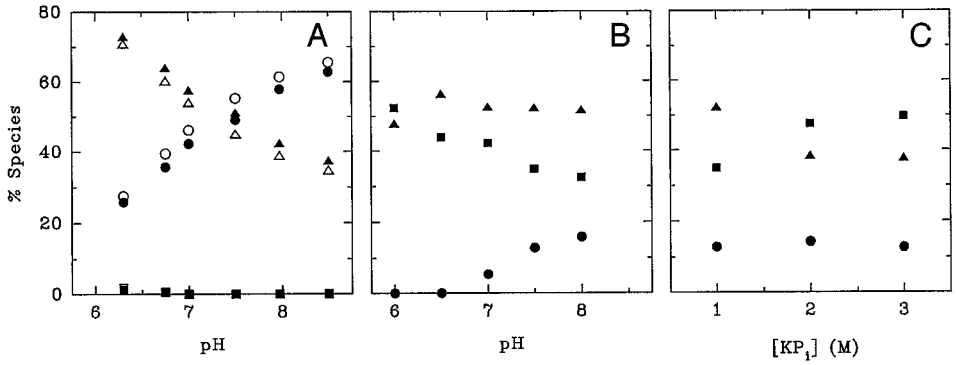


FIG. 5. **Dependence on pH and phosphate concentration of the fraction of high spin aquomet, high spin pentacoordinate, and low spin hemichrome for crystalline and soluble oxidized HbI.** The fractions of high spin hexacoordinate (△, ▲), high spin pentacoordinate (○, ●), and low spin hemichrome (□, ■) species were calculated by a linear combination of the basis spectra as described under "Materials and Methods". *Panel a*, crystalline HbI; *open* and *closed symbols* refer to data recorded along the *a* and *b* crystal axes, respectively. *Panel b*, soluble HbI in 1 M phosphate buffer. *Panel c*, soluble HbI in phosphate buffer, pH 7.5.

amount of hexacoordinate heme is essentially constant over the pH range studied. In 3 M phosphate, namely at an ionic strength approaching that of the crystal suspending medium, the amount of hemichrome is significantly higher than in 1 M phosphate (Fig. 5*c*).

The polarization ratio for oxidized HbI crystals was calculated from the reference spectra at pH 8.5 (Fig. 2*a*) either at 602 nm or at 500 nm. At these wavelengths, which correspond to the absorbance maxima of the pentacoordinate and hexacoordinate high spin components, respectively, the heme behaves as a planar absorber (25). The PR values obtained, 2.4 and 2.3, respectively, differ considerably from the value characteristic of the ferrous protein.

## DISCUSSION

Allosteric transitions of oligomeric proteins within the crystal lattice are usually limited by intermolecular interactions that stabilize a particular conformational state. This is the case for human hemoglobin A, Hb Rothschild, and des-Arg Hb, crystallized from polyethylene glycol solutions, that remain in the T state upon oxygenation (14–20). However, when trigonal crystals of *Escherichia coli* aspartate carbamoyltransferase in

the T state are soaked in a solution containing the substrate L-aspartate and phosphate, a slow molecular transition to the R state takes place, suggesting a kinetic rather than a thermodynamic barrier between the two conformations (27). Furthermore, in crystals of tetrameric L-lactate dehydrogenase from *Bifidobacterium longum*, grown from a solution where the R state conformation prevails, lattice forces favor a 1:1 mixture of T and R state molecules, the latter ones binding a substrate analog (28).

Activity measurements have provided an independent criterion to establish whether and to which extent lattice interactions affect symmetry and regulation of some oligomeric proteins. Glyceraldehyde-3-phosphate dehydrogenase from lobster muscle retains in the crystalline state the negative cooperativity ("half-of-the-sites reactivity") exhibited in solution in the reaction with the chromophoric acylating reagent $\beta$-(2-furyl)acryloylphosphate (29–31). The tryptophan synthase $\alpha_2\beta_2$ complex from *Salmonella typhimurium* maintains the reciprocal regulation of ligand binding and catalytic activity of the $\alpha$ and $\beta$ sites mediated by intersubunit interactions (32, 33). On the other hand, the asymmetric environment of the two chemically equivalent subunits of aspartate aminotransferase from chicken heart mithochondria within triclinic crystals causes a kinetic asymmetry in the reaction with natural substrates that has no counterpart in solution (34).

Suspensions of cross-linked microcrystals of rabbit muscle phosphorylase *a* showed homotropic cooperativity in the reaction involving a fixed concentration of glucose 1-phosphate and variable concentrations of maltoheptose (Hill coefficient in the crystal $n_H = 1.08$ *versus* 1.17 in solution) but not in other reactions (35). HbI represents a most favorable study case as it fully retains positive homotropic ligand binding cooperativity in crystals of the quality used for x-ray studies. The structure of liganded HbI presently available has been determined using crystals belonging to the monoclinic C2 space group (1–4), whereas the structure of deoxy-HbI has been determined using crystals belonging to the orthorhombic $C222_1$ space group (2, 3). The observed conformational differences between the liganded and the unliganded states of HbI involve small changes in the relative position of the two subunits (3.3° rotation and 0.4 Å translation) with striking changes in the heme environment. These include sinking of the heme groups 0.6 Å deeper into the subunits due to the extrusion of Phe-97 from the proximal side of the heme pocket into the subunit interface. The movement of one heme alters the hydrogen bond network that links the heme propionates to F helix residues (*i.e.* Lys-96 and Asn-100) of the other subunit, thus increasing its oxygen affinity. It will be of interest to compare these conformational differences with those occurring in orthorhombic crystals grown in the deoxy state and exposed to increasing oxygen pressure, in order to verify whether some of them may simply be due to different lattice contacts.

The oxygen affinity measured along the two orthogonal axes is the same. Since the contribution of the two hemes to polarized light absorption is different along the two crystal axes (Table I), this result indicates that, within experimental error, the two hemes possess the same oxygen affinity and, hence, that the monoliganded intermediates cannot be distinguished.

The comparison of the polarization ratios of liganded and unliganded HbI provides information on a possible reorientation of the heme upon oxygenation. The similarity of the PR values (1.79–1.81) indicates that ligand binding is not accompanied by a heme tilt, in agreement with the existing crystallographic evidence (1–4). The observed PR value for deoxy-HbI (1.79) is lower than that (2.0) calculated from the x-ray coordinates of the deoxy molecule, assuming a rigid heme plane. In all myoglobin and hemoglobin crystals, the observed PR value is consistently lower than the calculated value, due to fluctuations of the heme that produce an apparent out-of-plane (*z*-polarized) component in the heme absorption (36).

For oxidized HbI crystals, the PR value (2.3–2.4) observed at pH 8.5 differs from that characteristic of reduced HbI crystals and can be attributed to a different heme orientation. Although the available data do not allow one to estimate the extent of rotation, even a tilt of a few degrees would be expected to involve appreciable conformational changes in the surrounding globin, due to the tight packing of the heme inside the protein. Indeed, in the crystal, oxidation of reduced HbI induces the development of fine cracks, which rapidly disappear, while, in solution, the transition from reduced to oxidized HbI causes quaternary changes that ultimately lead to dissociation of the dimer into the monomeric, low spin hemichrome (*M*). The dissociation equilibrium in solution involves also two spectroscopically distinct dimeric species, a hexacoordinate aquomet ($D_h$) and a pentacoordinate ($D_p$) component, according to the scheme: $M \rightleftarrows D_h \rightleftarrows D_p$. As described by Spagnuolo *et al.* (21), the amount of $D_h$ is essentially constant between pH 6.5 and 8.0 and over the ionic strength range 0.01–0.1 M. The monomeric hemichrome is favored by acid pH and higher ionic strength, while the pentacoordinate species prevails at alkaline pH and at low ionic strength. The monomerization process occurs in solution even under solvent conditions approaching those of the crystal mother liquor. In contrast, in the crystal the dimeric pentacoordinate form is stabilized over the whole pH range studied, whereas the monomeric hemichrome formation is absent due to lattice forces that drastically shift the equilibrium toward the right. Thus, HbI crystals provide an interesting example of the balance between lattice energies and energies involved in tertiary and quaternary rearrangements of multisubunit proteins. Lattice interactions that do not restrict the large tertiary and subtle quaternary conformational changes associated with cooperative oxygen binding are strong enough to impair the quaternary transition that would lead to dissociation of the oxidized protein into monomers.

REFERENCES


1. Royer, W. E., Jr., Hendrickson, W. A. & Chiancone, E. (1989) *J. Biol. Chem.* **264,** 21052–21061
2. Royer, W. E., Jr., Hendrickson, W. A. & Chiancone, E. (1990) *Science* **249,** 518–521
3. Royer, W. E., Jr. (1994) *J. Mol. Biol.* **235,** 657–681
4. Condon, P. J. & Royer, W. E., Jr. (1994) *J. Biol. Chem.* **269,** 25259–25267
5. Royer, W. E., Jr., Love, W. E. & Fenderson, F. F. (1985) *Nature* **316,** 277–280
6. Rupley, J. A. (1969) in *Structure and Stability of Biological Macromolecules* (Timasheff, S. N., and Fasman, G. D., eds) pp. 291–352, M. Dekker, New York
7. Makinen, M. W. & Fink, A. L. (1977) *Annu. Rev. Biophys. Bioeng.* **6,** 301–343
8. Rossi, G. L. (1992) *Curr. Opin. Struct. Biol.* **2,** 816–820
9. Rossi, G. L., Mozzarelli, A., Peracchi, A. & Rivetti, C. (1992) *Philos. Trans. R. Soc. Lond. A* **340,** 191–207
10. Haurowitz, F. (1938) *Z. Physiol. Chem.* **234,** 266–274
11. Perutz, M. F. (1953) *Acta Crystallogr.* **6,** 859–864
12. Monod, J., Wyman, J. & Changeux, J.-P. (1965) *J. Mol. Biol.* **12,** 88–118
13. Perutz, M. F. (1970) *Nature* **228,** 726–734
14. Brzozowski, A., Derewenda, Z., Dodson, E., Dodson, G., Grabowski, M., Liddington, R., Skarzinski, T. & Vallely, D. (1984) *Nature* **307,** 74–76
15. Liddington, R., Derewenda, Z., Dodson, G. & Harris, D. (1988) *Nature* **331,** 725–728
16. Liddington, R., Derewenda, Z., Dodson, E., Hubbard, R. & Dodson, G. (1992) *J. Mol. Biol.* **228,** 551–579
17. Mozzarelli, A., Rivetti, C., Rossi, G. L., Henry, E. & Eaton, W. A. (1991) *Nature* **351,** 416–419
18. Rivetti, C., Mozzarelli, A., Rossi, G. L., Henry, E. & Eaton, W. A. (1993) *Biochemistry* **32,** 2888–2906
19. Rivetti, C., Mozzarelli, A., Rossi, G. L., Kwiatkowski, L., Wierzba, A. M. & Noble, R. W. (1993) *Biochemistry* **32,** 6411–6418
20. Kavanaugh, J. S., Chafin, D. R., Arnone, A., Mozzarelli, A., Rivetti, C., Rossi, G. L., Kwiatkowski, L. D. & Noble, R. W. (1995) *J. Mol. Biol.* **248,** 136–150
21. Spagnuolo, C., De Martino, F., Boffi, A., Rousseau, D. L. & Chiancone, E. (1994) *J. Biol. Chem.* **269,** 20441–20445
22. Chiancone, E., Vecchini, P., Verzili, D., Ascoli, F. & Antonini, E. (1981) *J. Mol. Biol.* **152,** 577–592
23. Dvorak, J. A. & Stotler, W. F. (1971) *Exp. Cell. Res.* **68,** 144–148
24. Hofrichter, J. & Eaton, W. A. (1976) *Annu. Rev. Biophys. Bioeng.* **5,** 511–560

25. Eaton, W. A. & Hofrichter, J. (1981) *Methods Enzymol.* **76,** 175–261
26. Ikeda-Saito, M., Yonetani, T., Chiancone, E., Ascoli, F., Verzili, D. & Antonini, E. (1983) *J. Mol. Biol.* **170,** 1009–1018
27. Gouaux, J. E. & Lipscomb, W. N. (1989) *Proc. Natl. Acad. Sci. U. S. A.* **86,** 845–848
28. Iwata, S., Kamata, K., Yoshida, S., Minowa, T. & Otha, T. (1994) *Nature Struct. Biol.* **1,** 176–185
29. Berni, R., Mozzarelli, A., Pellacani, L. & Rossi, G. L. (1977) *J. Mol. Biol.* **110,** 405–415
30. Vas, M., Berni, R., Mozzarelli, A., Tegoni, M. & Rossi, G. L. (1979) *J. Biol. Chem.* **254,** 8480–8486
31. Mozzarelli, A., Berni, R, Rossi, G. L., Vas, M., Bartha, F. & Keleti, T. (1982) *J. Biol. Chem.* **257,** 6739–6744
32. Ahmed, S. A., Hyde, C. C., Thomas, G. & Miles, E. W. (1987) *Biochemistry* **260,** 5492–5498
33. Mozzarelli, A., Peracchi, A., Rossi, G. L., Ahmed, S. A. & Miles, E. W. (1989) *J. Biol. Chem.* **264,** 15774–15780
34. Kirsten, H., Gehring, H. & Christen, P. (1983) *Proc. Natl. Acad. U. S. A.* **80,** 1807–1810
35. Kasvinsky, P. J. & Madsen, N. B. (1976) *J. Biol. Chem.* **251,** 6852–6859
36. Ansari, A., Jones, C. M., Henry, E., Hofrichter, J. & Eaton, W. A. (1993) *Biophys. J.* **64,** 852–868

**Cooperative Oxygen Binding to *Scapharca inaequivalvis* Hemoglobin in the Crystal**

Andrea Mozzarelli, Stefano Bettati, Claudio Rivetti, Gian Luigi Rossi, Gianni Colotti and Emilia Chiancone

*J. Biol. Chem. 1996, 271:3627-3632.*
*doi: 10.1074/jbc.271.7.3627*